EXPERIMENTAL TESTS OF THE MACH EFFECT THRUSTER

H. Fearn and K. Wanser

California State University Fullerton, Physics Department,
800 N. State College Blvd. Fullerton, CA 92834, USA.
hfearn@fullerton.edu , kwanser@fullerton.edu

The Mach Effect Thruster (MET) is a device which employs Mach's principle and utilizes fluctuations in the internal energy of an accelerating object to produce a steady linear thrust. There are many versions of Mach's principle[1], here we take the definition which states that the inertia of a body is due to the gravitational interaction with all matter and energy flow in the universe. These accelerating objects are stacks of PZT (lead zirconium titanate) crystals, which are powered by an AC voltage. The theory predicts that the thrust produced in the device is proportional to dP/dt, where P is the power supplied. In this paper we test whether a DC voltage switched on/off may generate thrust with no AC frequency present in the power supplied to the device.

I. INTRODUCTION

In 1953, Dennis Sciama published a paper, "On the Origin of Inertia" in the Monthly Notices of the Royal Astronomical Society[2] wherein he resuscitated Einstein's idea[3] that the inertia of material objects should be accounted for by a field interaction with the chiefly distant matter in the cosmos. He did not use Einstein's theory of gravity, general relativity theory, to convey the interaction. Rather, he proposed a vector theory of gravity modeled on Maxwell's formalism for electrodynamics. Eventually, it was recognized that the vector formalism (first mentioned by Heaviside[4]) was just an approximation to Einstein's general relativity theory. But the simplicity and transparency of the vector formalism made plain what was involved in explaining inertial effects as gravitational interactions with chiefly distant "matter" in the universe. There is now a well established Maxwell like formalism of Einstein's general relativity which is capable of addressing very accurately many of the problems treated with the theory[2-10]. In this paper we use the linearized version of general relativity commonly called the parametrized post Newtonian (PPN) approximation for flat space time and weak gravitational fields present therein. At the most elementary level, if we seek to show that inertial effects are the consequence of the gravitational action of chiefly distant matter in the cosmos, we must show that when a "test particle" is accelerated by an "external" force, the action of gravity due to all of the "matter" in the cosmos just produces the reaction force that opposes the external accelerating force required by Newton's third law of mechanics. In this paper it is assumed that the Sciama results hold[1,8]. If that is true, and the theory is locally Lorentz invariant, then we can be confident that all of the inertial effects of classical mechanics will follow.

II. MACH DEVICE THEORY

The theory will be derived here in an approximate and hopefully transparent manner. It is a little different from previous derivations since it begins with the modified PPN[5-7] wave equation for the gravitational field. The modified version allows for the body to be moving at velocity v, not static[7]. A more rigorous derivation will be given elsewhere, this is meant to be more insightful and simplified.

Woodward[11,12] has previously derived his wave equation from a divergence of the 'inertial' reaction to a 4-force. This can easily be explained as follows, and is similar to the explanation given by the mechanics text book by Marion[13] . In flat space-time Newton's force law holds approximately. Newton's second law says that the acceleration of a test mass near the center of a dust cloud is radially inward, hence we may write,

$$\vec{g} = -\nabla f \qquad [1]$$

Here $\vec{g}$ is the force per unit mass of the test body. The rate of change of "separation acceleration" between nearby radially separated dust particles is given by,

$$\nabla \cdot \vec{g} = -4pGr \qquad [2]$$

This is similar to the differential form of Gauss's law for electric field $\nabla \cdot \vec{E} = 4pr$ where r is the charge density. We have the tidal force per unit mass around the test body given by,

$$\nabla^2 f = -\nabla \cdot \vec{g} = 4pGr \qquad [3]$$

This divergence represents the gravitational field around the particle. This is similar to how Woodward derived his force per unit mass wave equation. He actually re-derived the Einstein equation, in a flat space time, using 4-vector notation rather than the simplified 3-vector notation used here. The $\vec{g} = -\nabla f$, here corresponds to Woodward's f, a force per unit mass 4-vector, he then derived his wave equation for density fluctuation from the time part, energy stress tensor term, which is essentially energy density. In the process he showed that to make the mass fluctuate you need to apply an external force, which causes the body to accelerate and deviate from its intended geodesic. Here, we will start from the point of view of standard the PPN wave equation and develop the same ideas.
Using the flat metric[6] h_{aa}= (1,-1,-1,-1), we define $\varphi = \frac{GM}{R}$, to agree with Woodward[11] , the interval squared as,

$$ds^2 = g_{\alpha\beta} dx^\alpha dx^\beta$$

and the modified metric as[7],

$$
\begin{aligned}
g_{00} &= (1-\frac{2\varphi}{c^2}) \\
g_{ij} &= -(1+\frac{2\varphi}{c^2})\delta_{ij} \\
g_{0i} &= 4\frac{\varphi}{c^2}\frac{\upsilon}{c}
\end{aligned} \qquad [4]
$$

Then the small perturbation form the flat metric is given by $h_{\mu\nu}$ which is defined by the following[5-7],

$$
\begin{aligned}
g_{\mu\nu} &= \eta_{\mu\nu} + h_{\mu\nu} \\
\bar{h}_{\mu\nu} &= h_{\mu\nu} - \frac{1}{2}\eta_{\mu\nu}h \\
h &= h^{\alpha}_{\alpha}
\end{aligned} \qquad [5]
$$

Einstein's field equation in linearized form becomes[5,6]

$$
(-\frac{1}{c^2}\frac{\partial^2}{\partial t^2}+\nabla^2)\bar{h}^{\mu\nu} = -16\pi G\frac{T^{\mu\nu}}{c^4} \qquad [6]
$$

The standard definition for the energy-stress tensor of a perfect fluid as defined by MTW[5], using proper velocity $u^{\mu} = (\gamma c, \gamma\vec{v})$ and pressure P,

$$
\begin{aligned}
T^{\mu\nu} &= (\rho(\vec{r},t)+\frac{P}{c^2})u^{\mu}u^{\nu} + Pg^{\mu\nu} \\
T^{00} &= (\rho(\vec{r},t)+\frac{P}{c^2})u^{0}u^{0} + Pg^{00} = (\rho(\vec{r},t)+\frac{P}{c^2})\gamma^2 c^2 + P \\
\sum_i T^{ii} &= \sum_i \left[(\rho(\vec{r},t)+\frac{P}{c^2})u^{i}u^{i} + Pg^{ii}\right] = (\rho(\vec{r},t)-\frac{P}{c^2})\gamma^2 u^2 - 3P
\end{aligned} \qquad [7]
$$

The $\rho(\vec{r},t) = \rho_0(\vec{r}, t \pm R/c) + \rho_u$ is the density of the device plus the density of the universe respectively. The density of the universe spatially uniform and is very small, of the order 10^{-28} kg m^{-3} and the density of the device is of order 10^{4} kg m^{-3}.

Taking the diagonal trace of the energy-stress tensor[14] and considering a time dependent mass density we get,

$$
\begin{aligned}
\sum_{\alpha} T^{\alpha\alpha} &= \gamma^2\rho(\vec{r},t)\left(1+\frac{u^2}{c^2}\right)+\gamma^2 P\left(1-\frac{u^2}{c^2}\right) - 2P \cong \rho(\vec{r},t) - P \\
&= \rho_u c^2 + \rho_0\left(\vec{r}, t \pm \frac{R}{c}\right)c^2 - \left(\frac{\partial\rho_0}{\partial t}\right)^2\frac{R^2}{\rho_0} \\
&= \left[\rho_u + \rho_0(\vec{r}) \pm \frac{R}{c}\left(\frac{\partial\rho_0}{\partial t}\right) + \frac{1}{2!}\left(\frac{R}{c}\right)^2\frac{\partial^2\rho_0}{\partial t^2} \pm \ldots\right]c^2 - \left(\frac{\partial\rho_0}{\partial t}\right)^2\frac{R^2}{\rho_0}
\end{aligned} \qquad [8]
$$

The term in the square bracket is a Taylor expansion of the device density only $\rho_0(\vec{r}, t \pm R/c)$ but the R/c term is time dependent and can become large, in fact R can become the Hubble radius, the size of the causal universe. All these terms are dimensionally correct for energy density. The pressure term comes from purely dimensional analysis allowing only the mass to change with time. We have taken the velocity of the device to be small and so $\gamma = 1$.

Consider that the energy density of the device is being exchanged with that of the universe. This expansion represents a radiation type term. The density of the universe is not expanded since it is already small. The universe density is very small and the universe density fluctuations (needed to conserve energy) are spread over too wide a volume and as such are negligible. The mass fluctuations of the device are considered to be very small, an equivalent mass fluctuation on a universal scale would be unnoticeable. We assume our device is positioned at the centre of the universe and the majority of the universal mass can be considered, simply, as a spherical shell of matter at the Hubble radius away[3]. The last term is a pressure term solely dependent on rate of change of mass. If we allow for both retarded and advanced waves, then the first derivative term will cancel out.

Now we substitute the trace of the energy stress tensor into Eq.(6) along with the diagonal h^{00} and h^{ii} components for the weak field. This gives,

$$\begin{aligned}\frac{1}{c^2}\frac{\partial^2 \phi}{\partial t^2} - \nabla^2 \phi &= 2\pi G\left[\rho_0(\vec{r},0) + \frac{1}{2}\left(\frac{R}{c}\right)^2 \frac{\partial^2 \rho_0}{\partial t^2}\right] - 2\pi G\left(\frac{\partial \rho_0}{\partial t}\right)^2 \frac{R^2}{\rho_0 c^2} \\ &= 2\pi G\left[\rho_0(\vec{r},0) + \delta\rho_0(\vec{r},t)\right]\end{aligned} \qquad [9]$$

Where we have neglected the energy density of the universe in comparison with the device locally. This allows us to identify a transient term,

$$\delta\rho_0(\vec{r},t) = \frac{1}{2}\left(\frac{R}{c}\right)^2 \frac{\partial^2 \rho_0}{\partial t^2} - \left(\frac{\partial \rho_0}{\partial t}\right)^2 \frac{R^2}{\rho_0 c^2} \qquad [10]$$

If we take $\rho_0(\vec{r},t) = \varepsilon_0 / c^2$ where $\varepsilon_0(\vec{r},t)$is the energy density contained in the device, then the transient mass-density can be written as,

$$\delta\rho_0(\vec{r},t) = \frac{R^2}{2c^4}\frac{\partial^2 \varepsilon_0}{\partial t^2} - \left(\frac{\partial \varepsilon_0}{\partial t}\right)^2 \frac{R^2}{\rho_0 c^6} \qquad [11]$$

Using the definition from Cook[9], $2\pi G \rho_0 R^2 = c^2$ where R is the radius of the causal universe, which corresponds to Woodward's[11,12] use of $2\pi\phi = c^2$ (without the 2**π**) we obtain,

$$\delta\rho_0(\vec{r},t) = \frac{1}{4\pi G}\left[\frac{1}{\rho_0 c^2}\frac{\partial^2 \varepsilon_0}{\partial t^2} - \frac{2}{(\rho_0 c^2)^2}\left(\frac{\partial \varepsilon_0}{\partial t}\right)^2\right]. \qquad [12]$$

Integrating the power over the volume the oscillating mass V, and introducing the power *P* supplied to the device we get,

$$\delta\rho_0(t) = \frac{1}{4\pi G}\left[\frac{1}{V\rho_0 c^2}\frac{\partial P}{\partial t} - \frac{2}{(\rho_0 c^2)^2}\left(\frac{P}{V}\right)^2\right], \qquad [13]$$

where $\frac{P}{V} = \frac{1}{V}\int \frac{\partial \varepsilon_0}{\partial t}\, d^3x$ the *P/V* is the average power over the device.

Finally integrating over the volume of the mass to which the power is applied we finally obtain

$$\delta m_0(t) = \frac{1}{4\pi G}\left[\frac{1}{\rho_0 c^2}\frac{\partial P}{\partial t} - \frac{2}{(\rho_0 c^2)^2}\frac{P^2}{V}\right], \qquad [14]$$

which is the form of Woodward's mass change formula[8,9] . Note that the mass of the device is taken as $m(t)=m_0 + \delta m_0(t)$. P is the spatially averaged power over the device. The first term in the rate of power change results in gravitational waves and gives thrust for the Mach effect thruster (MET) device. The second term (wormhole term) associated with pressure, caused by the mass fluctuation, is always negative. This term may be the basis for generating negative energy density for stable wormhole construction. The mass fluctuation predicted only occurs in an object that is being accelerated as the power fluctuates. If there is no "bulk" acceleration there is no mass fluctuation.

The mass fluctuation does not lead to changes in the rest masses of elementary particles. The work done by the external force (non gravitational) deposits energy in the bonds that bind the particles together, not the particles themselves. Specifically, in lead-zirconium-titanate (PZT) the resulting realignment of the atomic dipoles leads to a mechanical expansion or contraction of the PZT material. The acceleration dependence can be restored to Eq. (14) by noting that when a net external force *F* acts on a body the change in energy *dW* of the body is *dW= F.dx*. So the rate of change of energy, or power

$P=dW/dt= F.\upsilon_{cm}$. Furthermore, the rate of change of power, $dP/dt = F \cdot a_{cm} + \upsilon_{cm} \cdot \dot{F}$, where υ_{cm} is the relative velocity of the centre of mass (COM) of the system. So our changing mass formula becomes, using the net external force *F* (here not gravitation ie. electrostriction and/or piezoelectric force),

$$\delta m_0(t) = \frac{1}{4\pi G}\left[\frac{1}{\rho_0 c^2}\frac{\partial P}{\partial t}\right] \approx \frac{1}{4\pi G \rho_0 c^2}\left(F \cdot a_{cm} + \upsilon_{cm} \cdot \dot{F}\right)$$

$$\delta m_0(t) = \frac{1}{4\pi G \rho_0 c^2}\left(m\, a_{cm}{}^2 + \dot{m}\upsilon_{cm} \cdot a_{cm} + m\, \upsilon_{cm} \cdot \dot{a}_{cm}\right) \qquad [15]$$

Evidently the simplest Mach effect depends on the first term, the square of the acceleration of the body in which it is produced. Changing mass systems are known to allow for acceleration of the COM without violation of momentum conservation[15]. We do not address the subtleties of the work energy theorem for variable mass systems in the present work[16]. We also intend to re-derive these equations using the gravitomagnetic (Maxwell like electric and magnetic fields) for gravitation. The radiation damping found in sections 65 and 75 of Landau and Lifschitz *Classical theory of fields* will be helpful here. (Look for a later article in this journal.)

Einstein recognised that Mach's principle was contained in his general relativity and was in fact guided by that principle. In Einstein's book, "The meaning of Relativity" Einstein says[17],

" The idea that Mach expressed, that inertia depends upon the mutual action of bodies, is contained, to a first approximation, in the equations of the theory of relativity; it follows from these equations that inertia depends, at least in part, upon mutual actions between masses… this idea of Mach's corresponds only to a finite universe, bounded in space, and not to a quasi-Euclidean, infinite universe."

III. EXPERIMENTAL SETUP

The idea is to test the hypothesis of Mach principle by producing a fluctuation in the mass of an object in the lab, use it to produce a steady thrust and match the theory with the experiment[11,12,15]. We push on the object (whose mass is fluctuating) when it is more massive and pull back when it is less massive, this produces a steady linear acceleration in the body, which is detectable in the laboratory. This steady force could be used to produce a propulsive force on a massive object without having to expel propellant from the object. This would be highly desirable from a space rocket point of view, which then would not have to carry a massive payload of expendable fuel.

The easiest way to produce rapid energy fluctuations is to apply high ac voltages to a stack of PZT dielectric crystals. See figure 1. below.

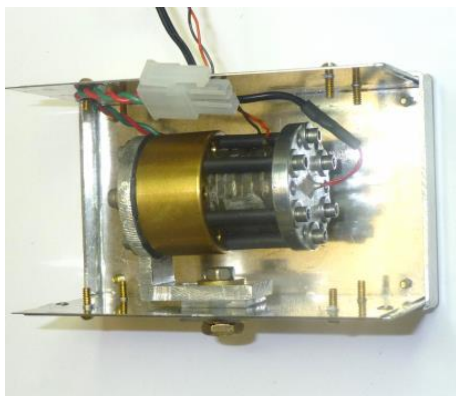

Fig. 1: A PZT stack device mounted in half of a Faraday cage. The Faraday cage sits on the end of a very sensitive torsion balance beam. Visible are the brass disc, the six 2-56 bolts covered with heat shrink for insulation, the PZT discs and aluminium end cap with embedded thermistor.

These crystals act as capacitors by storing energy in their dielectric core as they are polarized. The piezoelectric and electrostrictive properties force the crystals to deform (accelerate). The condition that energy vary with time is satisfied as the ions in the crystal lattice are accelerated by the changing external field. The assumption that all the energy delivered to the capacitors ends up as proper energy density is an optimistic assumption. These particular Steiner Martin (SM-111) crystals have a dissipation of approximately 0.4% due to heat loss.

Note too that simply charging and discharging a capacitor will not by itself, produce a Machian type mass fluctuation. The capacitor must also be undergoing a bulk acceleration of the kind produced by electrostriction and the piezoelectric effect.

The capacitor will however undergo the much smaller mass fluctuation due to special relativity $dm = de / c^2$.

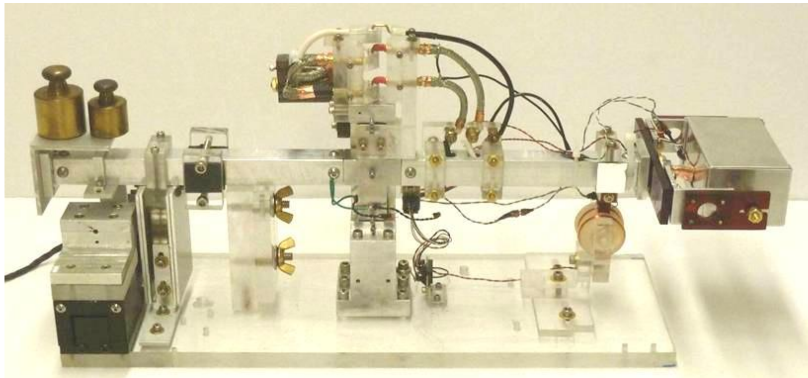

Fig. 2: The thrust balance used in the experiment whose results are reported here. C-flex flexural bearings in the central column support the balance beam which hangs from the top bearing. These bearings provide the restoring torque for thrust measurements. The position of the beam is sensed with a Philtec D63 optical position sensor which is attached to a stepped motor on the left of the beam.

In the work reported here, the device tested consisted of 8 discs of 2mm thick by 19mm diameter PZT crystals glued together with 1 embedded accelerometer. The accelerometer was made with two 0.3mm thick crystals which are located between the second and third PZT discs near the aluminium end cap. For testing, the crystals were clamped between thin 4.5mm thick aluminium cap and a thicker 16mm brass disk. The "L" shaped aluminium mounting bracket was 3mm thick. The device was bolted inside a Faraday cage which was then attached to the end of a sensitive torsion balance. See figure II. above. The electrodes between the crystal discs are hand cut from sheets of 50.5 μm brass sheet. A stack of brass sheets are clamped together and drilled with holes which helps with adhesion. They are then cut to size and sanded. The glue used is a 50:50 mixture of Versamid 140 and Shell Epon Resin 815C. All the positive contacts line up and all the accelerometer electrode positives line up separately and are separately soldered together to form electrode contacts that can be wired for power. For further experimental details of the electronics and calibration methods for the thrust balance we refer the reader to previous works[11,12.]

IV. EXPERIMENTAL PROCEDURE

The device was setup as in figures 1 and 2. If an MET device is operated at constant power, in a slight off resonant conditions, it will produce a steady thrust. This particular device had a preferred operating frequency of 39.5KHz. Each run consisted of taking data for 32 seconds. The first 6 seconds were quiescent data to establish the background noise. This was followed by 14 seconds of a single frequency 39.5KHz voltage of around 200 volts, followed by the remaining 12 seconds of quiescent data. Signal averaging was performed by taking a dozen runs under exactly the same circumstances and averaging them to supress random noise. In order to reduce spurious signals, runs were done with the device facing "forward" on the balance beam and then also "reversed". One can easily reverse the direction by rotation of the Faraday cage by 180 degrees.

The device is mounted inside the Faraday cage on the side wall so this does not effect the device mounting. The mount point is always on the side and is not switched from top to bottom. In which case the effects of gravitational torque on the mount point may need to be taken into account.

Once the forward and reversed runs are averaged they are differenced to produce a clear thrust signal where all non-reversing spurious thrust signals are cancelled. A sample data of forward, reversed and differenced is shown below. An example of a single forward run is shown in Fig 3, below. Minimal averaging over 3 or 4 runs only has taken place. The blue line represents the applied voltage, the red line is the thrust measured by the optical probe. The voltage from the probe has been converted into a measure of thrust shown on the left scale. Note that in figures 3(a) and (b) the baseline is lower after the power pulse than before. This is not as marked in figure 4 where the data is differenced not averaged. If a comparison is made with previous results[12], when the power pulse was only applied for 1 or 2 seconds, this baseline drop is larger than that previously shown. The baseline does return to pre-pulse values after a few more seconds, which we could not show due to restrictions in our data acquisition system.

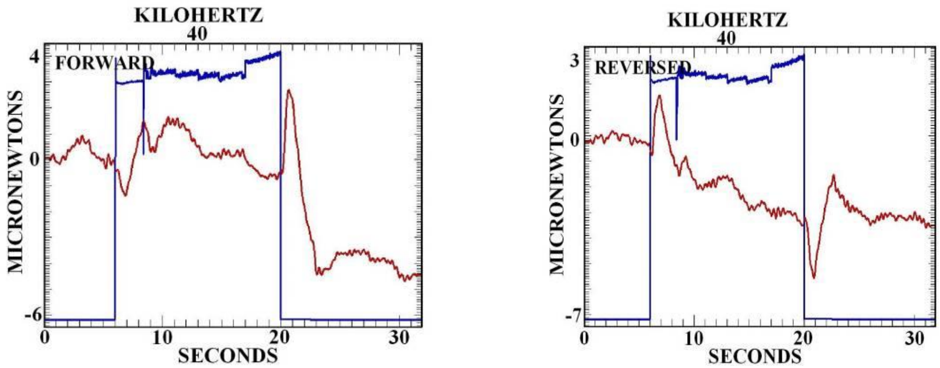

Fig. 3(a) and (b): Predicted Mach effect thrust. The dark blue line is the voltage squared applied to the PZT stack at a frequency of 39.5KHz. The red line indicated the thrust as measured by the optical probe. The power comes on at 6 seconds, stays on for 14 seconds and is then switched off. Note the red line moves upward in (a) left, showing maintained thrust for the 14 second power duration. Also note the switching transient which gives a slightly higher thrust momentarily as the AC voltage is switched on and off. Notice that in the plot on the right, the reversed data (b), the red line drops for 14 seconds then picks up again after pulse ends.

The data for the reversed runs is shown in Fig 3(b). Note the direction of the red line for thrust is now reversed. Below is the differenced data, figure 4, where we have subtracted reversed data from the forward data to get a much clearer signal. All the non-reversing spurious signals have been removed by this subtraction process.

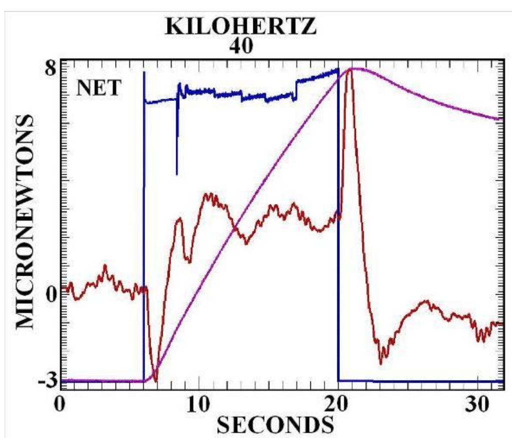

Fig. 4: Differenced Data: Forward minus reversed data. The dark blue line is the voltage squared applied to the PZT stack. The red line indicated thrust and the magenta line is the heat as measured by the thermistor embedded in the end aluminium cap of the device. The temperature change here is about 4 °C. Note the steady heating during the 14 seconds of steady thrust. The thrust is seen by the red line moving upward above the noise level for the 14 seconds of the applied AC voltage of about 200V. We see about 3 μN of thrust.

The switching transient thrusts deserve special attention.

Switching Transients

The switching transients appear to give a much higher thrust than the steady value, seen in Figs 3 (a) and (b) as the red line, between the on-off of the voltage signal. When the power is switched on, the rate change of power (*dP/dt*) rapidly increases, then it reaches a maximum as the PZT stack charges up the first time. This is the transient zone with a large impulse thrust. The *dP/dt* becomes steady and no longer changes with time, this is where we reach the steady thrust of the device, represented by an approximate horizontal line displaced from the quiescent noise level. (The line becomes more horizontal when several runs are averaged together.) Note that the transient thrust is in opposite directions for the turn-on and turn-off, of the device. These transients also reverse for forward and reverse device directions. It may be possible to utilise these transients as the main trust component with clever "fixing" of the phase of the input signal. This is a topic for further experimentation. The input power rise time was between 13-30ms, quite slow. This would allow for 1200 cycles or so of the input signal voltage which has a period of approximately 25 μ s (for frequency 40kHz.)

Thermal Effects

Qualitatively, the switching transients can be explained by both Mach and thermal effects, as both effects display dependence on the rate of change of the power applied to the device, *dP/dt,* where *P* is the power. Thermal effects, in this case, can be excluded on two grounds. First, they are more than an order of magnitude smaller than the effects seen. The temperature rise in the device during a run is typically only four degrees centigrade. Secondly, the thermal linear expansion coefficient, in the direction of the polarization, of PZT along the axis of the device is very small. We note that one paper[18] quotes the linear expansion as positive $6.8\text{x}10^{-6}$ K^{-1} and the thermal expansion in the radial direction, perpendicular to the polarization direction, is negative (it shrinks radially). Another paper gives the radial linear thermal expansion coefficient[19] of PZT is -0.55 $\text{x}10^{-5}$ K^{-1}.

Experimentally this is not correct for a stack under preload. Our data shows that the stack actually shrinks in the longitudinal direction and expands slightly radially which is exactly the reverse of what these papers say. One should note here that the thermal expansion coefficient is highly composition dependent, and it also has a history. The first heating showing markedly different thermal expansion than subsequent. One also must take into account bolt preloading which has a substantial effect on the thermal expansion. A simple hypothesis, which will be tested further, is that since the aluminium end cap and brass reaction mass have thermal expansion coefficients of 22.2 $\text{x}10^{-6}$ and 18.7 x 10^{-6} m/(m-K) respectively and the stainless steel bolts have a thermal expansion of 16.0 x 10^{-6} m/(m-K) the PZT is being compressed between them. The aluminium end cap and the brass are expanding and the stainless steel bolts are holding them in place so they are both pushing against the PZT stack and forcing it to contract. We have found, by experimentally heating the stack at the ground contact that during the run the compressed stack actually shrinks in size lengthwise and therefore shows a negative thermal expansion at room temperature or just above. The negative thermal expansion is what we see during a normal 14 second run discussed here. Only when the device heats by several degrees centigrade then the PZT starts to expand.

When the device is mounted inside the Faraday cage, the small linear fluctuation in the device has no effect on the balance beam. The torsion balance measures linear thrust only not oscillatory behaviour inside the device itself.

The negative thermal expansion means that any "thrust" due to heating would be in the wrong direction to affect our experimental results. The heat during the thrust is steady. For the heating to produce thrust it must be changing rapidly and it is clear by the differenced data, shown below Fig 4., that this is not the case. The temperature has a straight line slope indicating steady heating not rapidly changing heating which would be an abrupt curve.

The expansion of the device is severely restrained due to force applied by clamping of the bolts. It is possible to estimate the stopping force, from known data[20], to be around 10,173 N. When this force is applied in compression by the bolts there will be zero motion of the PZT stack due to piezoelectric or heating effects. The force of the bolts maybe estimated from p12 of the bolt tightening handbook [21].

T » μFd, is the torque and T = 4 inch-pounds, μ is the coefficient of friction for steel on brass,

μ=0.2, F is the force in pounds, d is the diameter of the bolt. (We have ignored the pitch angle as small). Each of our 2-56 bolts with a diameter of 0.0860in compress the stack with a force of 232.6 lbs or equivalently 1034.8N per bolt. (Using conversion 1 lb = 0.4536 Kg). For 6 bolts that is 6209.0 N more than 1/2 the stopping force. If there is any motion at all it will be a magnitude smaller than the observed thrust signal.

The preload (tension due to bolts) also affects the piezoelectric and electrostrictive expansion and contraction of the PZT so that the stack length (or excursion) of the device may be calculated as

$$x = x_0 + Nf(K_p V + K_e V^2) \quad [16]$$

where x_0 is the actual length of the PZT stack, N is the number of PZT discs in the stack, K_p and K_e are the piezoelectricand the electrostrictive constants and f is the preload fraction which we need to determine experimentally. Previously[11,12], we had used x_0 instead of the Nf term which gave us an underestimate. We need x to calculate the acceleration and force on the stack.

A calibration of the optical probe was done to find the absolute excursion of the PZT due to expansion, not heating, just piezoelectric expansion. The method was as follows. The device was mounted on an optical breadboard outside the vacuum chamber. The device could not physically move, it was bolted down with ¼ inch bolts. The optical probe was mounted on the same breadboard on top of a very fine adjustment linear stage. The optical probe was facing the polished aluminium end cap of the device and about 0.5mm away from it. Without powering the device, measurements were taken of the voltage from the optical probe when the probe was moved through 1 fine adjustment of 2 μm of the linear stage. A dozen or more voltages were taken for an average result. It was found that a 1.4 V change in sensor voltage corresponded to 1 μm change in position of the probe from the end of the device. The device was then powered and we looked at the power spectrum at the near resonant frequency of 39.5KHz. The power change when the device was running was on average y=-34.7 dB which gives an average (dozen runs) of 18mV. (Using $y=10 \log_{10} x$, where $x = V^2$). Since we found 1.4V per 1μm that implies that the maximum excursion due to the piezoelectricity is on the order of 13 nm , this is with the regular preload from the bolts holding the device together.

Spurious Electromechanical effects

Another possibility is that instead of the desired Mach effect we may be seeing some "poorly characterized" spurious electromechanical effect. The question can be raised.

"*Do the thrusts seen simply result from an impulsive displacement of the centre of mass of the PZT stack when the power is switched on, that is locked by unspecified means until the power is switched off ?*"

One of the unspecified proposals is the anharmonicity of the voltage signal. That is the voltage signal is asymmetric, leading to the device spending more time, say, extended than contracted. Were this true, the blue trace in the oscilloscope plot below, Fig 5., (voltage blue, accelerometer yellow) would be markedly asymmetric with respect to the horizontal hashed central zero line on the scope.

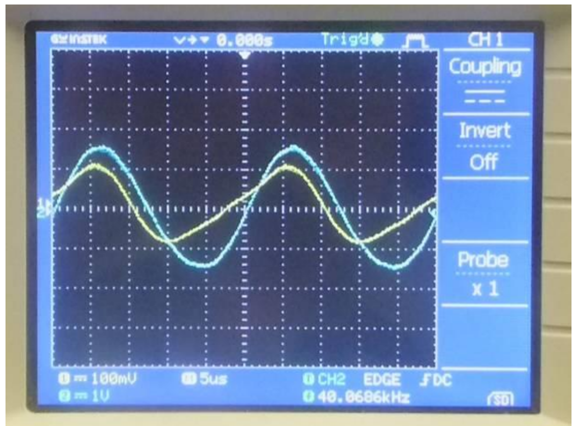

Fig. 5: Oscilloscope Trace. Photo of oscilloscope during a run showing thrust. The blue line is the voltage applied, 200V at 39.5KHz. The yellow line is the accelerometer trace. Note that the traces are roughly symmetrical about the zero line.

<u>DC Voltage Tests</u>

Another possibility is that the switch on/off of the power is causing a lock up of the device and the appearance of thrust. This matter can be easily answered by modifying the power circuit so that a DC voltage can be applied for say 10 or 11 seconds and we can look for thrust when there is no driving resonant frequency. Since the AC driving voltage was around 200 V, a DC voltage of about 125V should be sufficient for this test. An average of 125 volt DC was applied for 11 seconds. The device in forward position was run over 150 times to collect a good sampling of data. We ran the device with +125V and then switched the polarity to -125V in the same direction and then did the same in reversed direction. The results averages are presented below in Fig 6.

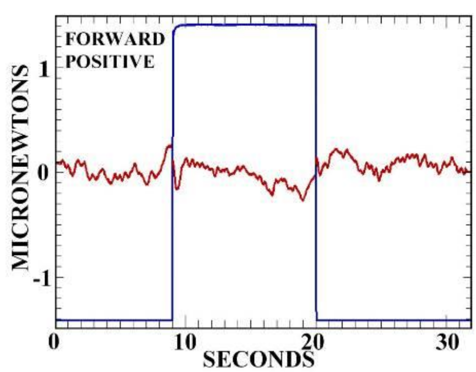

Fig 6.(a) Forward data runs for +125 Volts DC. (Averaged data of 150 runs.) Applied for 11 seconds. Rise time 30ms. Blue line is voltage squared, red line indicates thrust or lack thereof.

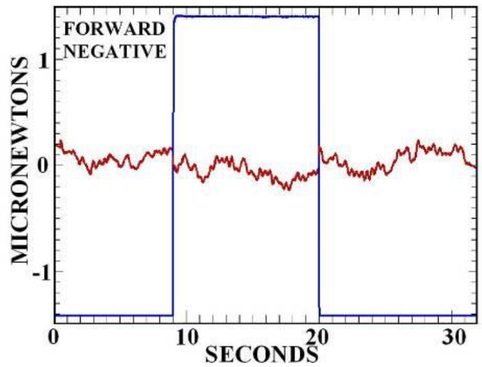

Fig 6. (b) Forward runs with -125Volts DC applied for 11 seconds. (Averaged data 150 runs). The rise time 30ms. Blue line is voltage squared, red line indicates thrust or lack thereof

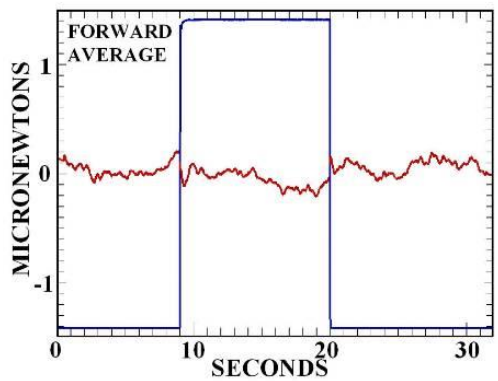

Fig 6.(c) Forward runs all averaged, both polarities. ±125 volts DC applied for 11 seconds. 30ms rise time. (Averaged data 300 runs).

Clearly there is no thrust seen in any of the forward data sets or the averaged set. The same was found to be true in the reversed data sets which we do not show here since they look the same as the forward runs. Then we averaged the data from the forward and reversed directions and found something interesting in the differenced data of the averaged runs.

See figure 7 (a) and (b) below. During the experiment HF removed a coil from the circuitry and managed to reduce the rise time to 13ms. This had no effect on the results shown here.

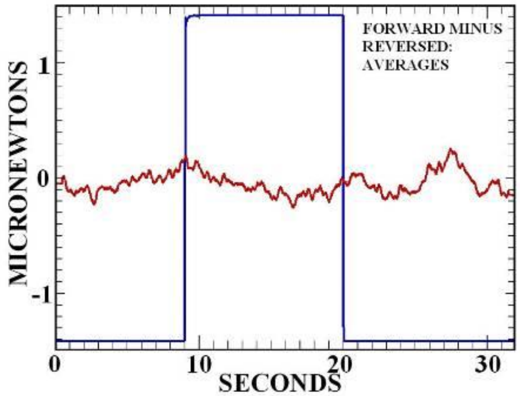

Fig. 7.(a) Forward minus Reversed data. (Averaged 300 runs.) The average of all the reversed runs (both polarities) was subtracted from the average of all the forward runs. We see no thrust. 125 V applied for 11 seconds with 30ms rise time. Blue line is the applied, voltage squared, the red line indicates thrust signal.

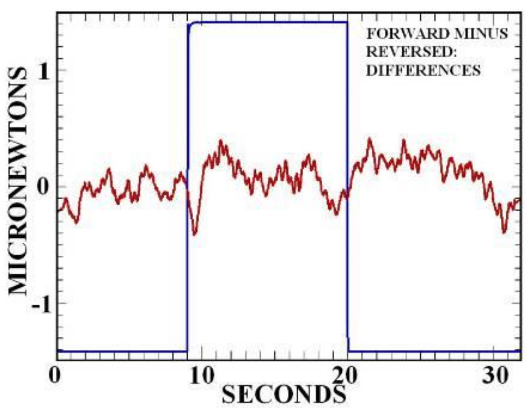

Fig. 7. (b) Forward minus Reversed Differences. (Average of 300 runs).
The difference was taken between the + and - polarity in the forward direction. The difference was taken of the different polarities in the reversed direction. Then the two differences were subtracted from each other. Now we regain a very small transient thrust signal at switch on and switch off. This is much smaller than the regular thrust signals seen since the vertical scale has changed from 5 to 1. (See figures 3, 4 and 5 for the different scale used.)

If the switched AC thrusts are actually produced by the Mach effect, then one might well ask why no thrust effect is present in the differenced averages in figure 7(a). The reason is that the Mach effect depends on *dP/dt*, rate of change of power. When the voltage is switched on (or off) the rate of power exchanged increases to a maximum ($dP/dt > 0$) then decreases ($dP/dt < 0$) as the capacitor becomes fully charged. The same is true when the power is switched off. So the *dP/dt* cancel out when the device is switched on and off and there is no net thrust. The large thrust signal is only present when AC voltage is used because *dP/dt* is either greater than zero or less than zero throughout each transient.

V. CONCLUSIONS

General relativity encompasses Mach's principle- that inertial forces are due to the gravitational action of all the "matter" in the universe[1-3]. The rest mass fluctuations occur when a body is being accelerated by an external force and at the same time is undergoing energy changes in its internal structure[11,12]. These rest mass fluctuations can be combined with an external force (like extension of a piezoelectric material by applying a voltage) in Mach effect thrusters (METs).

In section IV we explained how thermal effects are of the wrong sign to account for the thrust seen. Available papers cited appear to give the wrong sign for the thermal expansion coefficient of PZT under preload, the expansion of the aluminium end cap and brass mass may be compressing the PZT since the bolts are holding them in place. Also it was shown experimentally that DC voltage switching does not provide any thrust, the AC near resonant frequency must be present. The crude MET demonstration presented earlier in section IV, shows a clear thrust signal, see Fig 4., that is MET's actually work.

VI. ACKNOWLEDGEMENTS

We thank the Aerospace Corporation team at El Segundo CA, headed by Greg Meholic, for taking the trouble to assess our work and for suggesting further tests to explore the nature of the effects seen. We also thank J. F. Woodward for help in producing the data and results reported here. Finally we thank the referee for interesting comments regarding the variation of internal energy and bulk acceleration, which we hope to explain more fully in a subsequent paper.

VII. REFERENCES

[1] C. Rovelli, *Quantum Gravity*, (Cambridge Univ. Press 2004). Page 76, definitions 1,7 & 8.

[2] D. W. Sciama, "On the Origin of Inertia", Mon. Not. R. Astron. Soc. **113,** p34 (1953)

[3] A. Einstein, ``Is there a Gravitational Effect which is Analogous to Electrodynamic Induction ?", Vierteljahrsschrift fur gerichtliche Medizin und offentliches Sanitatswesen **44,** 33-40 (1912). Translated into English and republished in the *Collected Works of Albert Einstein*, (Princeton Univ. Press 1996), (**CPAE**) vol. **4**. Doc. 3. p126.

[4] O. Heaviside, *Electromagnetic Theory*, Vol. **1**. Appendix B, (London, Ernest Benn Limited, 1893).

[5] C. W. Misner, K. S. Thorne and J. A. Wheeler, *Gravitation*, W. H. Freeman and Co. N.Y. (1973). Stress energy tensor is on p470.

[6] B. Schutz, *A first course in general relativity*, (Cambridge University Press 1985), pages 199-207 for h definition. Also same author Am. J. Phys. **52,** pp412-419 (1984).

[7] K. Nordtvedt, "Existence of the Gravitomagnetic Interaction", Int. Journ. of Theo. Phys, **27,** (11) 1395-1404 (1988).

[8] E. G. Harris, "Analogy between general relativity and the electromagnetism for slowly moving particles in weak gravitational fields", Am. J. Phys. **59**, (5) pp421-425 (1991).

[9] R. Cook, "Is gravitation a result of Mach's Inertial Interactions?", Nuovo Cimento **35**, 25 (1976).

(Other authors have slightly different numerical factors, this is model dependent.)

[10] J-F Sanchez, “The harmonic gauge condition in the gravitomagnetic equations”, arXiv:gr-qc/001007.

[11] J. F. Woodward, *Starships and Stargates*” (Springer Press, Dec 2012).

[12] H. Fearn and J. F. Woodward, “Recent results of an investigation of Mach Effect thrusters”, 48th Joint Propulsion Conference, Atlanta Georgia, 29th July -1st Aug 2012. Proceedings Published by AIAA, American Inst. of Aeronautics and Astronautics.
See also, H. Fearn and J. F. Woodward, “Experimental Null test of a Mach effect thruster”, arXiv:1301:6178. Published in, J. of Space Exploration vol. **2,** issue 2 p 98-105 (2013). URL http://www.mehtapress.com/mehtapress/Journals/Journal-of-Space-Exploration/Volume-2-Issue-2/Experimental-null-test-of-a-Mach-effect-thruster.html

[13] J. B. Marion & M. Thornton, *Classical Dynamics of Particles and Systems*, 4th Ed. (Harcourt College Pubs. 1995). pp199-201. See also. Maurice J. Dupre, “The Einstein equation and the energy density of the gravitational field”, arXiv:0803:1684. See also, Dupre, “The fully covariant energy momentum stress tensor of the gravitational field and the Einstein equation for gravity in general relativity”, arXiv:0903:5225.

[14] M. Kutschera, “Monopole gravitational waves from relativistic fireballs driving gamma-ray bursts”, Mon. Not. Roy. Astron. Soc. **345**, L1-L5 (2003).

[15] K. Wanser, “Center of mass acceleration of an isolated system of two particles with time varyiable masses interacting with each other via Newton’s third law inertial forces”, J. of Space Exploration, vol. **2.** (2) pp121-130 (2013). (Note Eq. (21) needs a factor of ½). URL http://www.mehtapress.com/mehtapress/Journals/Journal-of-Space-Exploration/Volume-2-Issue-2/Center-of-mass-acceleration-of-an-isolated-system-of-two-particles-with-time-variable-masses-interacting-with-each-other%20vi.html

[16] J. Copeland, “Work-energy theorem for variable mass systems”, Am. J. Phys. **50,** pp599-601 (1981).

[17] A. Einstein, *The Meaning of relativity*, Princeton Science Library, Princeton Univ. Press, 2nd Ed. Reprinted 2005. (Pages 100-108). Quotation from pages 107 and 108.

[18] Material Properties from Piezo Technologies. http://www.piezotechnologies.com/Ceramics/quick-selection-chart.aspx See also, B. Noheda et. al. , J. Mater. Sci. Lett. **16**, pp101-103 (1997).

[19] H. Navirian, D. Schick, P. Gaal et. al. “Thermoeleastic study of nanolayered structures using time-resolved x-ray diffraction at high repetition rate”, arXiv:1306.4165.

[20] Micromechatronics Inc. NEC/TOKIN actuators data sheets. http://www.mmech.com/tokin-actuators

[21] SKF (2001) , *Bolt Tightening Manual*, http://www.skf.com/files/880426.pdf